ISBN: 978-3-95450-132-8 doi:10.18429/JACoW-IPAC2014-TUOCB03

PERFORMANCE OF ELLIPTICAL POLARIZATION UNDULATORS AT TPS

T.Y. Chung, C.H. Chang, C.Y. Wu, J.C. Huang, F.Y. Lin, J.C. Jan, C.H. Chang, C.S. Hwang,
National Synchrotron Radiation Research Center, Hsinchu, Taiwan

Abstract

The design, assembly, magnet-block sorting, field shimming and performance of undulators of type APPLE-II in NSRRC are described. The mechanical error has been well controlled based on an optimized design and mechanical arts. Initial sorting of permanent magnets is developed to minimize effectively several adverse effects, such as magnetic inhomogeneities, imperfect geometry of blocks and mechanical frame issues, which challenge the sorting expectation, especially for an adjusted polarization undulator. The sorting algorithm shows a quantitative prediction of magnetic field and is verified by the results of measurements. A 2D virtual shimming algorithm was developed to optimize the field quality, including multipole and phase error, and the particle trajectory. We describe the considerations for each procedure and demonstrate the optimization, with measurement results.

INTRODUCTION

Undulators [1] of type APPLE-II have been extensively used as a source of polarized soft x-rays because of their widest range of tunable energy and greatest rate of polarization [2,3]. For these reasons, periods of two kinds and three elliptical polarization undulators (EPU) in total are under construction and will be installed in Taiwan Photon Source (TPS) in 2015. The characteristics and parameters of both EPU are organized in Table 1. As EPU48 has a larger deflection parameter than EPU46, it can attain a smaller energy than EPU46. Both EPU cover the K-edge absorption of the most abundant terrestrial elements (C, N, O, Si) and the L-edge absorption of the important transition metals (Fe, Co, Ni, Cu). Mechanical designs, manufacture and assembly of EPU48 are completed in NSRRC cooperating with domestic institutes. Inspection and correction of the magnetic field are also performed in NSRRC. For EPU46, a prototype is constructed by ADC. NSRRC continues the work to upgrade several mechanical parts and the control system, and also to complete shimming of the magnetic field.

Table1: TPS Phase 1 EPU Parameters

	EPU48 x2	EPU46
Photon energy /eV	230-2000	270-2000
Deflection parameter ky/kx	3.72/2.46	3.48/2.32
Period Length /mm	48	46
Number of periods	67	82
Total length /m	3.2	3.8
Range of magnet gap /mm	13≦G≦120	13.5≦G≦110

MECHANICAL STRUCTURE

The cast-iron support structure, instead of a welded structure, of EPU48 is designed to limit the effect of deflections and rotations of the magnet arrays [4], as seen in fig.1. The magnetic force acting on the magnetic girders has been calculated for each mode and is input into a finite-element mode of the EPU structure to optimize the supporter and the back beam. The entire and solid back beams supporting the magnetic girders are made of aluminium. The girder must be extremely rigid to prevent introduction of significant phase errors. Figure 2 shows the gap variation of supporters of various kinds and the back beam design in the horizontal linear mode. In this mode the vertical magnetic force can be as great as 34 kN at the minimum gap. The supporter, back beam, bearing and linear guide selection are all considered. As design optimization decreases the gap variation to ±3 μm, the contribution to the r.m.s. phase error is less than 0.5°. Major mechanical parts, including supporter, back beam, bearings, magnet girders and magnet holders have all been evaluated with a 50 % safety margin.

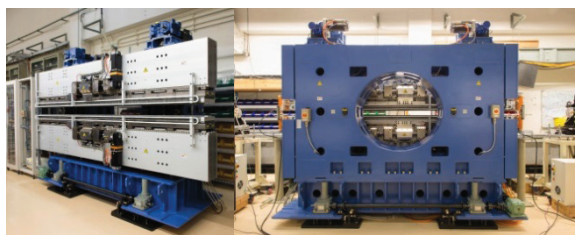

Figure 1: The front side of EPU48 is shown at the left, the rear side at the right.

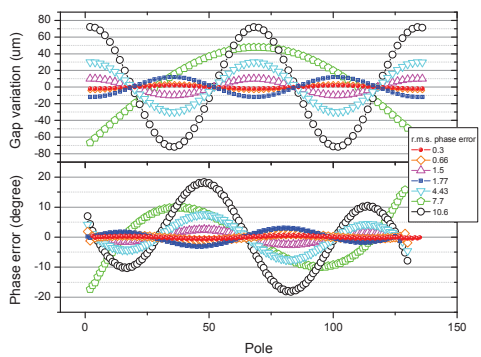

Figure 2: Gap variation of various kinds of mechanical design and the resulting phase error in horizontal linear mode.

ISBN: 978-3-95450-132-8 doi:10.18429/JACoW-IPAC2014-TUOCB03

After mechanical inspection and re-assembly, the gap variation is within ± 20 μm, corresponding to 3.4° phase error. The compensation of this error will be performed during magnet shimming using the movement of magnets. The repeatability of the gap and the phase movement are less than 2.5 μm, which ensures that a deviation of the photon energy is less than one tenth of the intrinsic width of the fifth harmonic.

MAGNETIC CONSIDERATIONS

Sorting of the magnet block is also carefully considered. Two stages are performed in our algorithm. In the first stage, individual blocks are sorted based on measurement with a Helmholtz coil. The components of magnetization of each magnet are imported into RADIA code [5] to minimize the phase error in various polarization modes; then 7 or 9 blocks are assembled into a submodule. We measured each submodule using a Hall probe and stretched wire. The goal is to eliminate the influence of inhomogeneity and imperfection of blocks. Figure 3(a) shows that measurement and simulation of distribution of the field on axis has no perceptible difference, but the field integral has a significant discrepancy, especially at the center of the magnets, as seen in Fig. 3(b). The practical measurements of each submodule data are input into our second stage of sorting code and are optimized based on simulated annealing [6].

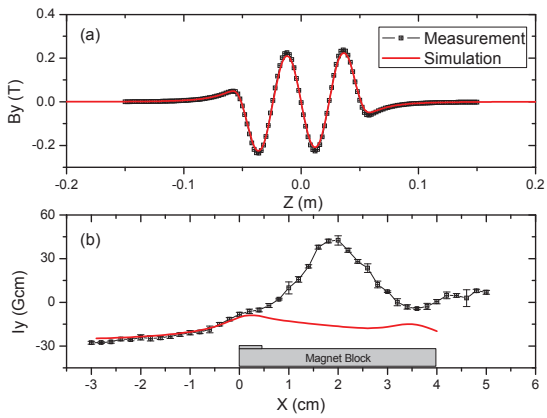

Figure 3:(a) Distribution of the field on the axis; (b) first field integral along transverse directions for one submodule with seven blocks.

The distribution of the deviation of first field integral of poles (d*I*/*I*) not only encompasses the superposition of each sub-module data but also considers the interaction nearby an interface. The interaction between submodules, which is attributed to a non-unit effect, is an important effect and has been considered in our sorting. Figure 4 shows d*I*/*I* of the expectation of our sorting and measurement. Apart from the interaction effect, obvious discrepancy exists between prediction and measurement. The contribution of the non-unit effect is periodic and up to 100 G cm. After the sorting, the phase error contributed from magnets is suppressed to that from mechanical error.

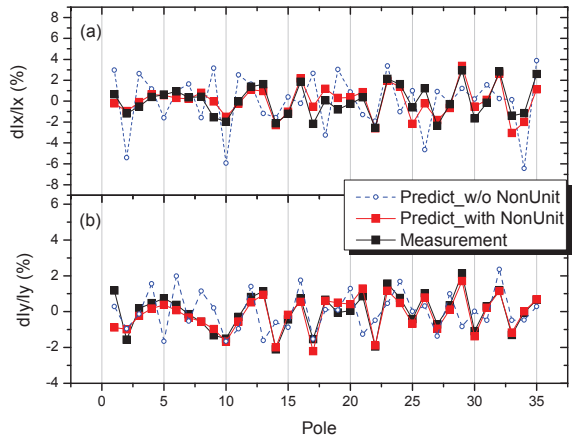

Figure 4: Distribution of deviation of first field integral of poles: (a) horizontal field; (b) vertical field.

OPTIMIZATION OF MAGNETIC FIELD

Despite the highly accurate mechanical manufacturing and careful consideration of magnet sorting, there remain some poles with a large deviation. Magnet blocks are moved about 0.1-0.2 mm to modulate the magnetic field via a screw-driven wedge and a slide mechanism, called virtual shimming [7]. A two-step shimming algorithm is developed to eliminate phase error and static multipole error. The goal of the first step is to improve the phase error. A decreased phase error has been shown to increase the straightness of a trajectory [8]. The influence of the movement of a magnet block on the magnetic field for all operational modes is considered; the suitable poles are selected in our shimming algorithm.

Figure 5 shows the results of straightness of horizontal and vertical trajectories in all operating modes. After the second stage of sorting, the straightness has been improved within ±11 μm. After shimming, it has even been improved within ±4 μm in all operating modes.

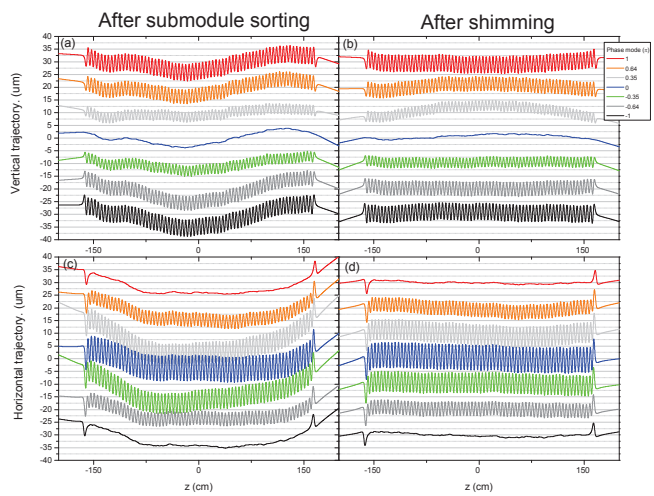

Figure 5: Straightness of (a,b) vertical and (c,d) horizontal trajectories; (a,c) before shimming, (b,d) after shimming.

After straightening of the on-axis trajectory, the r.m.s. phase errors for the horizontal/vertical linear polarization

ISBN: 978-3-95450-132-8 doi:10.18429/JACoW-IPAC2014-TUOCB03

modes of EPU48 and EPU46 are 2.4/2.3 and 3.8/2.9 at minimum gap 13/13.5 mm respectively. These results maintain a great spectral intensity, even for the energy at high harmonics. For example for EPU48, the flux density of the horizontal linear mode at the fifth harmonic energy is greater than 95 % of the ideal value, which is large enough to satisfy the users of soft X-rays.

Figure 6 shows a map of r.m.s. phase error of the APPLE-II EPU in several facilities. Constructing a longer and smaller gap of an undulator is difficult -- stiff mechanical structures and magnets of good quality are essential. Mechanical arts and treatment of magnetic field are equally important for a high-performance undulator.

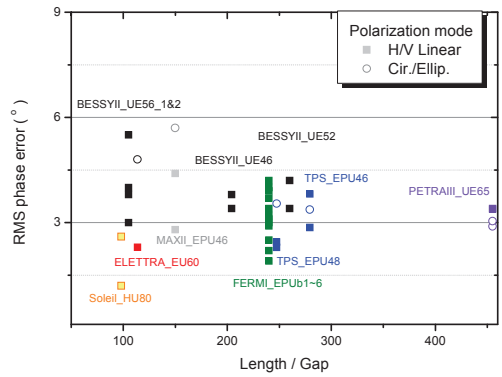

Figure 6: Map of r.m.s. phase error of APPLE-II EPU in several facilities.

Apart from decreasing further the phase error via virtual shimming, it is also possible to decrease multipole errors in our first stage of shimming. The deviation of the field integral is flattened, which means decreasing the quadrupole error, via selection of suitable poles.

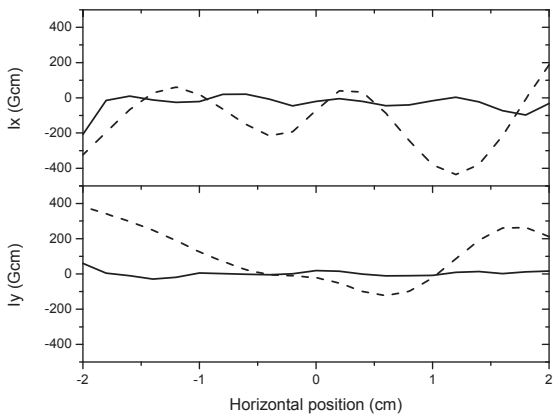

Figure 7: Field integral before (dashed line) and after (solid line) shimming at the minimum gap, 13 mm.

The second step of shimming is to decrease the residual field integral using magnet chips, called magic fingers, located at the extremities of EPU. The best arrangement of the chips is selected based on simulated annealing. Flattening of the field integral distribution is specifically optimized in the range ±15 mm. Figure 7 shows the horizontal and vertical field integrals at the minimum gap, 13 mm. After shimming, the static field integrals are flattened within ±30 G cm. Table 2 summarizes the multipole components for various polarization modes. All multipole terms are within our specification.

Table 2: Multipole Analysis of EPU48 for Each Phase Mode at gap 13 mm

Phase mode	Skew			
	Di.	Quad.	Sext.	Oct.
Vertical linear	-29	20	4	-12
Right circular	-46	-12	7	-1
Horizontal linear	-14	-6	-3	-3
Left circular	86	40	-22	-22

Phase mode	Normal			
	Di.	Quad.	Sext.	Oct.
Vertical linear	18	25	-19	-3
Right circular	-10	9	0	4
Horizontal linear	2	-3	-4	5
Left circular	34	21	-30	-3

CONCLUSION

The EPU48 are designed carefully and constructed completely in NSRRC. Sorting and shimming algorithms are developed based on a sequence of analysis of magnetic-field error, and separating the contribution of magnetic material and mechanical parts. The performance of an EPU48 is qualified to achieve the requirements of electron and photon beams.

REFERENCES

[1] S. Sasaki, “Analyses for a planar variably polarization undulator”, Nucl. Instrum. Methods Phys. Res. A, 347, 86. (1994).
[2] B. Diviacco *et al.*, “Design construction and field characterization of a variable polarization undulator for SOLEIL”, PAC 4242 (2005).
[3] J. Bahrdt *et al.*, “Magnetic field optimization of permanent magnet undulators for arbitrary polarization”, Nucl. Instrum. Methods Phys. Res. A, 516, 575. (2004).
[4] J. Bahrdt, “APPLE undulators for HGHG-FELs”, Proceeding of FEL, 521 (2006).
[5] http://www.esrf.eu/Accelerators/Groups/InsertionDevices/Software/Radia
[6] T. Y. Chung *et al.*, “Magnet-sorting Algorithm for an elliptically polarized undulator at TPS”, IEEE Transactions on Applied Superconductivity, 24 (3), (2014).
[7] S. Marks *et al.*, “The Advanced Light Source Elliptically Polarization Undulator”, PAC, 3221 (1998).
[8] R. P. Walker, “Phase errors and their effect on undulator radiation properties”, Phys. Rev. ST Accel. Beams 16, 010704 (2013).